

Enhanced Stability of Resonant Racetrack Plasmonic-Organic-Hybrid Modulators

Marco Eppenberger^{1*}, Bertold Ian Bitachon¹, Andreas Messner¹, Wolfgang Heni², David Moor¹, Laurenz Kulmer¹, Patrick Habegger², Marcel Destraz², Eva De Leo², Norbert Meier², Nino Del Medico², Claudia Hoessbacher², Benedikt Baeuerle^{2*}, Juerg Leuthold^{1,2*}

¹ETH Zurich, Institute of Electromagnetic Fields (IEF), 8092 Zurich, Switzerland

²Polariton Technologies AG, 8803 Rueschlikon, Switzerland

*Author e-mail addresses: marcoep@ethz.ch, benedikt@polariton.ch, leuthold@ethz.ch

Abstract: A high-speed and compact plasmonic organic racetrack modulator is shown to be orders of magnitude more robust against operating condition changes compared to resonant modulators based on the plasma dispersion effect while maintaining thermal tunability. Stable operation at 80°C is shown with no degradation. © 2022 Optica

Introduction

Microring modulators (MRM) are promising candidates for future communication networks due to their energy efficiency and small footprint needed for high spatial and spectral parallelization [1-3]. However, their temperature sensitivity pose a challenge [4] and require careful tuning of the operating point using control-loops to maintain the proper temperature of the ring cavity [5, 6]. In addition to environment temperature changes, MRMs are also sensitive to optical power variations [7] and driving power variations, which both generate heat in the cavity and hence change the ideal operating point. The operating laser power further gives rise to a large-signal hysteresis and non-linearity for wavelength tuning. Ultimately, the resonance wavelengths should be robust towards operating condition changes and still allow for thermal tuning, be it to compensate for fabrication imperfections or to track a drifting laser wavelength.

In this paper we compare a plasmonic organic hybrid (POH) racetrack (RT) modulator to two pn-junction based MRMs. We show a wavelength stability improvement of the POH modulator by up to 2 orders of magnitude if compared against the pn-junction MRMs. The POH RT modulator exhibits 250x less normalized wavelength shift under changing optical powers and up to 3000x less under changing driving RF power. Furthermore, we show that the modulator can operate at 80°C for extended time without any degradation or operation point drift.

Plasmonic-Organic-Hybrid Racetrack Modulator and pn-Junction Micro-Ring Modulators

The **plasmonic-organic hybrid modulator** is depicted in Fig. 1(a), see Refs. [8, 9]. The resonant modulator features 6.5 dB fiber-to-fiber loss and only 1.5 dB on-chip loss in its pass band and more than 110 GHz bandwidth at its 3 dB insertion loss (IL) point. The racetrack resonator is 80 μm in circumference. The device operates up to 220 Gbps 2PAM and 408 Gbps 8PAM transmission in a rack-to-rack-distance scenario [9]. This is one of the fastest ring modulators ever shown. The device was fabricated on the standard 220 nm silicon-photonic platform. Fig. 1(a) shows a sketch of the device on chip. For achieving intensity modulation, a plasmonic phase shifter with gold electrodes is included in the resonant part of a racetrack resonator realized with silicon waveguides (WG). The plasmonic phase shifter is activated with Lightwave Logic's Perkinamine™ chromophore series 3 [10]. The chromophores' orientation has been set with poling by an electric field near the material glass transition temperature T_g ($>170^\circ\text{C}$). At 1550 nm wavelength, the material's bulk r_{33} coefficient is 148 pm/V at 50% APC loading. The material achieved a stable performance at 85°C for over 2000 hours with less than 5% variance [11]. In Fig. 1(b) the

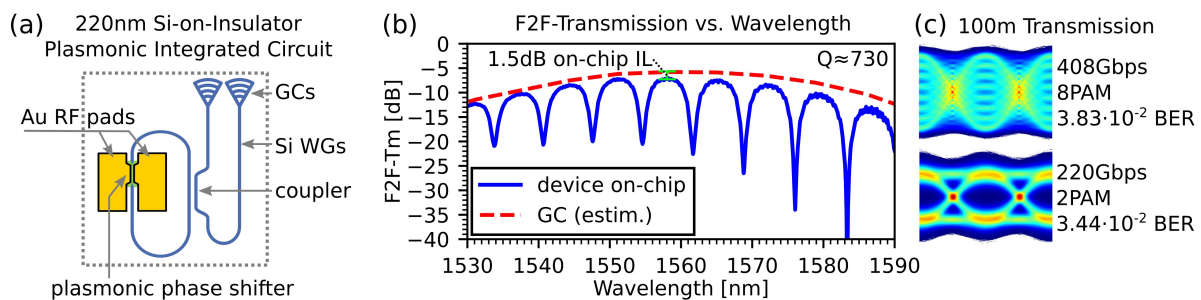


Fig. 1: (a) Schematic of the plasmonic-organic-hybrid (POH) racetrack (RT) modulator. (b) Static insertion-loss (IL) curve of the device and the grating-coupler (GC) losses. The device features an on-chip loss of 1.5 dB and a moderate Q-factor of 730. (c) Received eyes after 100 m transmission of intensity modulated signals. Figures adapted from [9].

static insertion loss characterization is shown. At the relevant operating resonance ($\lambda_r=1560$ nm), a 1.5 dB on-chip insertion loss is measured with a Q-factor of ~ 730 , a 19 dB ER resonance depth, 312 GHz full-width-half-max (FWHM), a tuning efficiency of 178 pm/V, an electro-optic bandwidth >110 GHz and a free spectral range of 7.16 nm. The device was put to test in a short-reach transmission scenario. See the received eye diagrams (differentially driven at $0.6 V_{p,50\Omega}$) in Fig. 1(c). More details on transmission experiment can be found in [9].

The two **pn-junction MRMs** have a $30 \mu\text{m}$ cavity circumference and interleaved silicon (Si) pn-junctions in the cavity for modulation. The Si MRM 1 was introduced in [12] ($\lambda_r=1171.8$ nm, Q-factor of 18800, 11 dB ER resonance depth, 13.6 GHz FWHM). The Si MRM 2 was introduced in [6, 13, 14] ($\lambda_r=1188.2$ nm, Q-factor 8400, 11 dB ER). Note that both Si MRM devices are close to what is being commercialized today [15] and hence were chosen as a valid baseline. Both MRMs are realized in an electronic-photonic monolithic integration platform [16]

Temperature and Power Stability of Resonant Modulators

When operating MRMs, their ideal operation wavelength for modulation is influenced by three factors: (i) Thermal environment [4], (ii) operating laser power [7] and (iii) electrical driving power. These three factors are now compared for POH RT and the two pn-junction based MRMs.

In Fig. 2, we show the absolute resonance wavelength shift $\Delta\lambda_r$ (a,c,e) and the $\Delta\lambda_r$ normalized to the resonator's width $\Delta\lambda_r / \text{FWHM}$ (b,d,f). As baseline served λ_r at 24°C , -15 dBm opt. power and no driving power. At each point, the λ_r was found by recording chip output power vs. wavelength followed by curve-fitting with a Lorentzian to enhance resolution where necessary. The normalized shifts are suitable for stability evaluation since they are directly proportional to the transmit-eye-closure.

We first investigate thermal tuning by changing the temperature of the devices by heating the chip with a thermo-electric element (TEC), Fig. 2(a), and find that the POH RT is equally tunable as the MRMs. We measure a temperature dependence of the resonance wavelengths of 54.9 pm/K for the POH RT, 57.8 pm/K for Si MRM 1 and 56.2 pm/K for Si MRM 2. The effect of the higher Q and shorter ring cavity can be best seen when plotting the resonance shift against the FWHM of the resonance, see. Fig. 2(b). The different geometries in the ring modulators length and Q-factor make the pn-rings by a factor 9 to 18 more prone to changes.

The optical power dependency is evaluated next, Fig. 2(c,d): we subject all modulators to optical powers from -15 dBm to 3 dBm (on-chip in waveguide before device). We find that the POH RT exhibits 250x less shift and is more optical power tolerant than both Si MRMs. A factor 9 and 18 could have been explained due to the different geometries. The unexpectedly high enhanced stability of the POH RT is attributed to the fact that light at worst dissipates in the plasmonic slot with the temperature stable material and not in the silicon waveguides.

Furthermore, the resonance wavelength depends on the electrical driving power, attributed to the ohmic losses in parasitic resistances in doped silicon. The driving power stability estimation, Fig. 2(e,f), is done by subjecting the modulators to different powers of a 10 GHz sine signal while scanning the wavelength. We find that the POH RT's are 10x to 3000x more stable to RF powers. Again, this is a way higher stability advantage over what would have been expected due to different geometries. We attribute this favorable performance to the plasmonic slot with almost purely capacitive parasitics whereas the Si MRMs' doped silicon have large resistive parasitics.

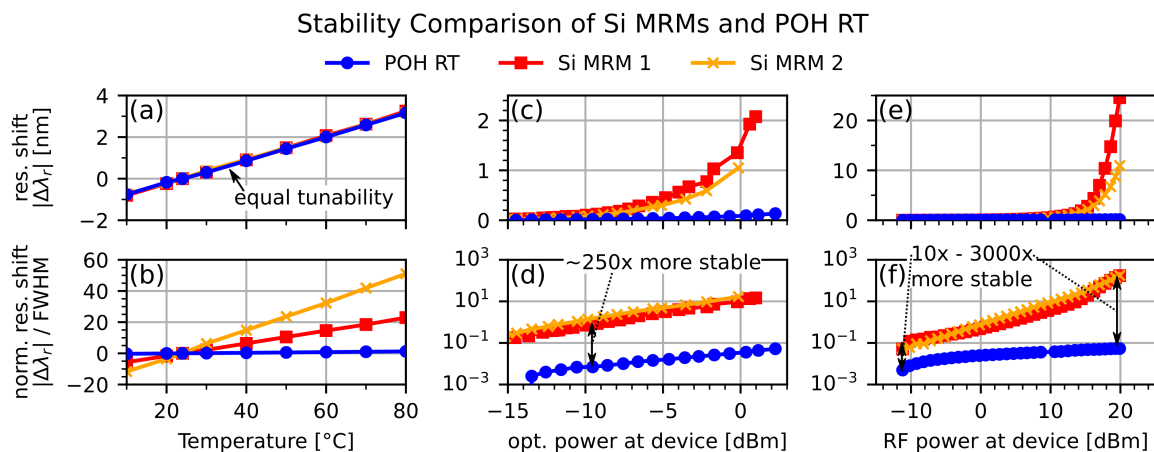


Fig. 2: Stability measurements comparing the POH-RT and two silicon (Si) microring modulators (MRM). The top row of the graphs shows the absolute change of resonance wavelength of the resonators, the bottom row the same change normalized to the resonator's full-width-half-max (FWHM). (a) and (b) investigate the chip temperature dependence, (c) and (d) the dependence on the optical power on-chip before the device, (e) and (f) the dependence on electronic signal driving power measured with a 10 GHz sine.

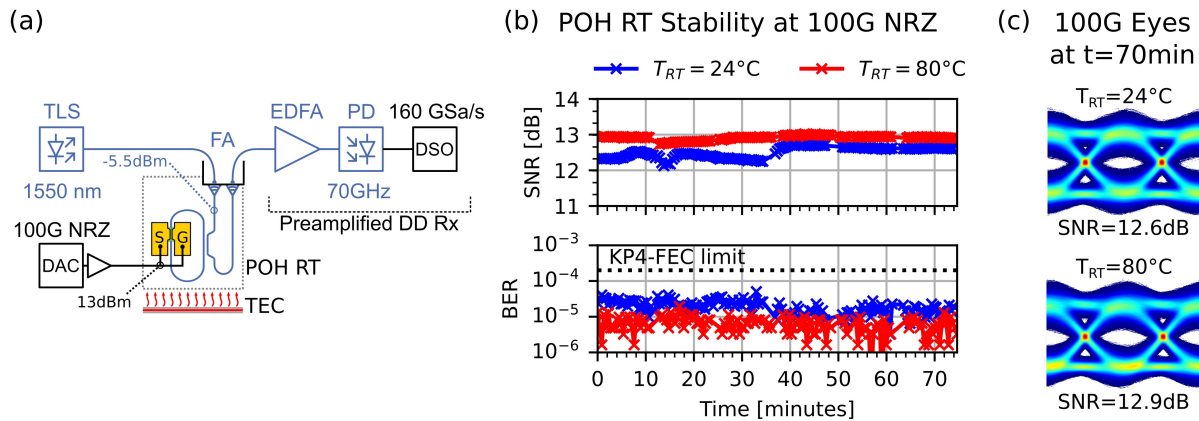


Fig. 3: Data transmission setup for transmission stability measurement. (a) Setup sketch of the device in the 100G NRZ transmission setup with POH RT operating points labelled. TECs are used to stabilize the chip at either 24°C or 80°C in an inert atmosphere. (b) BER and SNR time evolution for transmitting a 100G NRZ signal. BER and SNRs were evaluated every 10 seconds, the FA position was re-optimized every 10 minutes. (c) Eye diagrams after 70 mins of operation for both temps.

Operation of POH RT at Elevated Temperature

In a further study, we investigate the high-temperature capabilities of the POH RT. We test the stability of the operating point and the electro-optic performance at 24°C and at 80°C.

Fig. 3(a) shows the measurement setup and annotated operating conditions: We stabilize the POH RT at 24°C and at 80°C in an inert atmosphere with a TEC. We couple light from a tunable laser source (TLS) to the device and source the NRZ signal from a 100 GSa/s digital-analog-converter (DAC). We operate the device with a -5.5 dBm optical input power and 13 dBm electrical power. The signal is detected by a standard preamplified direct-detection (DD) receiver. We then use a minimal offline digital signal processing consisting of timing recovery, a 7-tap T/2-spaced equalizer followed by a hard bit decision and error counting.

In Fig. 3(b), we show the SNR and BER time evolution for the 100 Gb/s NRZ signal at both temperatures. We record the BER and the SNR every 10 seconds for more than 70 minutes. In both temperatures, the BER never exceeded the KP4 FEC limit. Due to setup drift, we re-optimized the fiber array (FA) location every 10 minutes while maintaining all other operating conditions. Fig. 3(c) shows the excellent eye diagrams of the last measured data point for both temperatures after 70+ minutes of operation. No degradation or drift in operating point was observed during this time.

Conclusion

We have shown that a plasmonic organic racetrack modulator is orders of magnitude more stable towards operating condition changes compare to that of Si MRMs. Stable operation at 80°C of the organic device was shown for more than 70 minutes.

Acknowledgements

ETH Zurich acknowledges funding by H2020 grants NEBULA and PlasmoniAC. Polariton Technologies AG thanks Lightwave Logic for the supply of the EO organic material. We thank the Binnig and Rohrer Nanotechnology Center (BRNC).

References

- [1] C. Sun, et al., *Nature* **528**, 534-538 (2015).
- [2] A. Melikyan, et al., *Opt. Express* **28**, 22540-22548 (2020).
- [3] S. Fatholouloumi, et al., *JLT*, 1-1 (2020), doi: 10.1109/JLT.2020.3039218.
- [4] W. Bogaerts, et al., *Laser & Photonics reviews* **6**, 47 - 73 (2012).
- [5] H. Li, et al., *JSSC* **50**, 3145-3159 (2015).
- [6] M. Eppenberger, et al., *JLT*, 1-11 (2021).
- [7] C. Sun, et al., *JSSC* **51**, 893-907 (2016).
- [8] A. Messner, et al., in *ECOC 2020*, doi 10.1109/ECOC48923.2020.9333272.
- [9] M. Eppenberger, et al., in *ECOC 2021*, PDP Th3C2.
- [10] Perkinamine 3 is a trade marked proprietary chromophore electrol-optic organic material developed at Lightwave Logic Inc.
- [11] M. Lebbby, in *ECOC 2019*.
- [12] L. Alloatti, et al., *Applied Physics Letters* **108**, 131101 (2016).
- [13] M. Eppenberger, et al., in *APC 2018*, p. JW21.3.
- [14] M. Eppenberger, et al., in *OFC 2021*, p. F2F.3.
- [15] M. Wade, et al., in *OFC2021*, p. F3C.6.
- [16] J. S. Orcutt, et al., *Opt. Express* **20**, 12222-12232 (2012).